Gas-Phase Molecular, Molecular Pair, and Molecular Triplet Fe^+ Affinities of Pyridines

Shuguang Ma, Philip Wong, Sheng Sheng Yang, and R. Graham Cooks*

Contribution from the Department of Chemistry, Purdue University, West Lafayette, Indiana 47907-1393

Received December 11, 1995[⊗]

Abstract: The relative molecular, molecular pair, and molecular triplet Fe^+ affinities of pyridines are determined by the kinetic method through examination of the competitive dissociation of Fe^+-bound dimer, trimer, and tetramer cluster ions. The molecular Fe^+ affinities vary strongly with the electron donating power of the substituent on the pyridine. Similar behavior is seen in the molecular pair and molecular triplet affinities, the first triplet affinity values determined by the kinetic method. The absolute Fe^+ affinity of pyridine itself is estimated to be 49 ± 3 kcal/mol. A linear correlation (slope = 0.38) is demonstrated between the relative Fe^+ affinities and the corresponding proton affinities of the meta- and para-substituted pyridines. The slope together with data from previous studies falls in the order of $OCNCO^+ \approx SiCl_3^+ > Cl^+ > CN^+ > SiCl^+ > Fe^+$, which indicates that the strength of binding to pyridines falls in the same order. The relative molecular pair and molecular triplet Fe^+ affinities also correlate linearly with the number averaged proton affinities of the pyridines. Lower than expected affinities are observed for systems containing ortho-substituted pyridines due to intramolecular steric effects between the ortho-substituted alkyl group(s) and the central Fe^+ cation. A set of gas-phase steric parameters (S^k), measured by the deviation of the experimental data from the regression line, shows much larger steric effects in the crowded trimers and tetramers.

Introduction

Gas-phase ion−molecule reactions between "naked" atomic metal ions and organic molecules have been increasingly investigated[1] since the first report of metal ion activation of saturated organic compounds in 1975 by Allison and Ridge.[2] Mechanisms for such processes have received much attention and two general mechanisms, oxidative addition[3−8] and remote functionalization,[9−16] have been proposed. The mass spectrometer has been widely used as an almost ideal instrument for the study of fundamental aspects of the chemistry of metal ions.[17,18] Perturbing influences due to solvation and ion-pairing are absent in the gas phase, and thus the intrinsic properties and reactivities of metal ions become accessible. In addition, the various mass spectrometric methods provide information on ion enthalpies, bond energies, and ion structures which can be compared directly with theoretical calculations.[1g]

Coordination complexes of transition-metal cations, M^+, with various inorganic and organic compounds have attracted interest as a source of fundamental thermodynamic information on metal−ligand bonding. Several powerful techniques have been developed to obtain bond energy information including guided ion-beam instruments,[19] Fourier transform ion cyclotron resonance mass spectrometry (FTICR-MS),[20] and triple-quadrupole mass spectrometry.[21] Techniques which contribute further to such thermochemical studies include the use of a reverse-geometry double-focusing mass spectrometer to measure the kinetic energy release distributions (KERD) associated with fragmentation,[22] photodissociation to measure the absolute metal−ligand bond energies,[23] and other methods including

[⊗] Abstract published in *Advance ACS Abstracts,* June 15, 1996.

(1) For reviews, see: (a) Schwarz, H. Acc. *Chem. Res.* **1989**, *22*, 282. (b) Eller, K. *Coord. Chem. Rev.* **1993**, *126*, 93. (c) Eller, K.; Schwarz, H. *Chem. Rev.* **1991**, *91*, 1121. (d) Allison, J. *Prog. Inorg. Chem.* **1986**, *34*, 627. (e) Armentrout, P. B.; Beauchamp, J. L. *Acc. Chem. Res.* **1989**, *22*, 315. (f) *Gas Phase Inorganic Chemistry*; Russell D. H., Ed.; Plenum: New York, 1989. (g) Freiser, B. S. *Acc. Chem. Res.* **1994**, *27*, 353. (h) Weisshaar, J. C. *Acc. Chem. Res.* **1993**, *26*, 213. (i) Martinho Simões, J. C.; Beauchamp, J. L. *Chem Rev.* **1990**, *90*, 629. (j) Armentrout, P. B. *Acc. Chem. Res.* **1995**, *28*, 430.

(2) Allison, J.; Ridge, D. P. *J. Organomet. Chem.* **1975**, *99*, c11.

(3) (a) Allison, J.; Ridge, D. P. *J. Am. Chem. Soc.* **1979**, *101*, 4998. (b) Allison, J.; Freas, R. B.; Ridge, D. P. *J. Am. Chem. Soc.* **1979**, *101*, 1332.

(4) (a) Beauchamp, J. L.; Steven, A. E.; Corderman, R. R. *Pure Appl. Chem. Soc.* **1979**, *51*, 967. (b) Armentrout, P. B.; Beauchamp, J. L. *J. Am. Chem. Soc.* **1981**, *103*, 784.

(5) Allison, J.; Ridge, D. P. *J. Am. Chem. Soc.* **1976**, *98*, 7445.

(6) (a) Freas, R. B.; Ridge, D. P. *J. Am. Chem. Soc.* **1980**, *102*, 7129. (b) Byrd, G. D.; Burnier, R. C.; Freiser, B. S. *J. Am. Chem. Soc.* **1982**, *104*, 3565.

(7) (a) Larsen, B. S.; Ridge, D. P. *J. Am. Chem. Soc.* **1984**, *106*, 1912. (b) Peake, D. A.; Gross, M. L.; Ridge, D. P. *J. Am. Chem. Soc.* **1984**, *106*, 4307.

(8) Burnier, R. C.; Byrd, G. D.; Freiser, B. S. *J. Am. Chem. Soc.* **1981**, *103*, 4360.

(9) Lebrilla, C. B.; Schulze, C.; Schwarz, H. *J. Am. Chem. Soc.* **1987**, *109*, 98.

(10) Lebrilla, C. B.; Drewello, T.; Schwarz, H. *J. Am. Chem. Soc.* **1987**, *109*, 5639.

(11) (a) Schröder, D.; Schwarz, H. *J. Am. Chem. Soc.* **1993**, *115*, 8818. (b) Schultz, R. H.; Armentrout, P. B. *J. Phys. Chem.* **1992**, *96*, 1662. (c) Hornung, G.; Schwarz, H. *J. Am. Chem. Soc.* **1995**, *117*, 8192.

(12) Karrass, S.; Eller, K.; Schulze, C.; Schwarz, H. *Angew. Chem., Int. Ed. Engl.* **1989**, *28*, 607.

(13) (a) Karrass, S.; Prusse, T.; Eller, K.; Schwarz, H. *J. Am. Chem. Soc.* **1989**, *111*, 9018. (b) Prusse, T.; Schwarz, H. *Organometallics* **1989**, *8*, 2851.

(14) Eller, K.; Lebrilla, C. B.; Drewello, T.; Schwarz, H. *J. Am. Chem. Soc.* **1988**, *110*, 3068.

(15) Steinrück, N.; Schwarz, H. *Organometallics* **1989**, *8*, 759.

(16) Schröder, D.; Zummack, W.; Schwarz, H. *J. Am. Chem. Soc.* **1994**, *116*, 5857.

(17) Armentrout, P. B. *Annu. Rev. Phys. Chem.* **1990**, *41*, 313.

(18) Heinemann, C.; Cornehl, H. H.; Schwarz, H. *J. Organomet. Chem.* **1995**, *501*, 201.

(19) (a) Armentrout, P. B.; Hodges, R. V.; Beauchamp, J. L. *J. Chem. Phys.* **1977**, *66*, 4683. (b) Armentrout, P. B.; Beauchamp, J. L. *J. Am. Chem. Soc.* **1981**, *103*, 784. (c) Armentrout, P. B.; Beauchamp, J. L. *J. Chem. Phys.* **1981**, *74*, 2819. (d) Armentrout, P. B.; Beauchamp, J. L. *J. Am. Chem. Soc.* **1981**, *103*, 6628. (e) Loh, S. K.; Hales, D. A.; Lian, L.; Armentrout, P. B. *J. Chem. Phys.* **1989**, *90*, 5466. (f) Schulz, R. H.; Armentrout, P. B. *Int. J. Mass Spectrom. Ion Process* **1991**, *107*, 29.

(20) (a) Marshall, A. G.; Grosshans, P. B. *Anal. Chem.* **1991**, *63*, 215A. (b) Forbes, R. A.; Lech, L. M.; Freiser, B. S. *Int. J. Mass Spectrom. Ion Processes* **1987**, *77*, 107.

(21) (a) McLafferty, F. W. *Science* **1981**, *214*, 280. (b) Sunderlin, L. S.; Wang, D.; Squire, R. R. *J. Am. Chem. Soc.* **1992**, *114*, 2788.

S0002-7863(95)04167-9 CCC: $12.00

ligand-exchange reactions and equilibrium measurements,[24] energy thresholds for endothermic reactions,[25] and ionization thresholds.[26]

The experiments described here seek information on the strength of binding of various pyridines with Fe^+. This system is chosen because of the long-standing interest in the use of Fe^+ as a chemical ionization reagent,[27] and the growing interest in the exploration of the structures of biological compounds using the dissociation of their metal-ion complexes.[28] The strength of the Fe^+−pyridine bond and the structural factors which control this bond strength might be representative of other metal−organic ligands in the rapidly growing field of metal-ion mass spectrometry.[1f,29] The experiments described here rely on the kinetic method,[30] which yields ligand binding energies from measurements of competitive ligand losses from a cluster ion by collision-induced dissociation (CID). For a weakly-bound cluster ion, monomer loss is the dominant channel, as illustrated in eq 1 in the case of a proton-bound dimer dissociating to give individual protonated monomers.

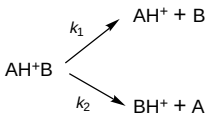

(1)

The rates of competitive dissociation, expressed as the relative abundances of the individual protonated monomers, can be used to determine the proton affinity difference between the two compounds, from

$$\ln\frac{k_1}{k_2} = \ln\frac{[AH]^+}{[BH]^+} = \frac{\Delta(PA)}{RT_{eff}} \qquad (2)$$

where $[AH]^+$ and $[BH]^+$ are the abundances of the two protonated monomers, ΔPA is the proton affinity difference between the two molecules A and B, and T_{eff} is the effective temperature of the proton-bound dimer. The derivation of this equation is presented elsewhere.[30,31]

Since the kinetic method is based on the assumption that entropy effects on fragmentation are negligible, it is best used for a pair of compounds with similar size and functional groups. The method yields proton affinities in good agreement with those from equilibrium measurements for carboxylic acids, alcohols, amines, and amino acids.[30−32] It has also been applied to order the relative Ag^+ affinities of alcohols,[33] the relative Ni^+, Co^+, and $CoCl^+$ affinities of nitriles[34] and alkylamines,[35] and the relative metal−ligand bond strengths in $ML_1L_2^+$ and $ML_1L_2L_3^+$ (M = Mn, Fe, Co and L = CO, NO, H_2O, and CH_3-OH, a case which shows synergistic ligand effects).[36] In work with a direct bearing on this study, Schwarz *et al.* have estimated the affinity of phenol for Fe^+ using the kinetic method.[37] The kinetic method has also been applied to the estimation of other metal ion affinities, including the relative Na^+ and Li^+ affinities of the 20 common amino acids by Bojesen and co-workers.[38] Recently, the relative Cu^+ affinities of the amino acids have been reported in a kinetic method study by Cerda and Wesdemiotis.[39] In addition, the method has been extended to estimate the proton affinities of phenoxyl and other free radicals,[40,41] the affinities of substituted pyridines toward Cl^+,[42] CN^+,[43] OC-NCO^+,[44] $SiCl^+$, $SiCl_3^+$,[45] and SF_3^+,[46] NH_4^+ affinities of crown ethers,[47] and NO_2^+ affinities of various organic ligands.[48]

In applying the kinetic method to the determination of Fe^+ affinities of a series of pyridines, a loosely-bound $Py_1Fe^+Py_2$ cluster ion is formed by the reaction of Fe^+ with a mixture of pyridines in the collision cell (Q2) of a pentaquadrupole mass spectrometer.[49] The Fe^+ affinities of pyridines are estimated by mass-selecting the dimers using Q3, dissociating them upon collision in Q4, and applying the relationship

$$\ln\frac{[Py_1Fe]^+}{[Py_2Fe]^+} = \frac{\Delta(Fe^+ \text{ affinity})}{RT_{eff}} \qquad (3)$$

Provided a loosely-bound dimer is formed between a pyridine and a reference compound with known Fe^+ affinity, it is possible to determine the Fe^+ affinities for the pyridine based on the

(22) Van Koppen, P. A. M.; Jocobson, D. B.; Illies, A.; Bowers, M. T.; Hanratty, M.; Beauchamp, J. L. *J. Am. Chem. Soc.* **1989**, *111*, 1991.
(23) Cassady, C. J.; Freiser, B. S. *J. Am. Chem. Soc.* **1984**, *106*, 6176.
(24) Uppal, K.; Lebrilla, C. B.; Drewello, T.; Schwarz, H. *J. Am. Chem. Soc.* **1988**, *110*, 3069.
(25) Armentrout, P. B.; Halle, L. F.; Beauchamp, J. L. *J. Chem. Phys.* **1982**, *76*, 2449.
(26) Murad, E. *J. Chem. Phys.* **1980**, *73*, 1381.
(27) (a) Peake, D. A.; Gross, M. L. *Anal. Chem.* **1985**, *57*, 115. (b) Peake, D. A.; Huang, S.-K.; Gross, M. L. *Anal. Chem.* **1987**, *59*, 1557. (c) Gross, M. L. *Acc. Chem. Res.* **1994**, *27*, 361. (d) Teesch, L. M.; Adams, J. *Org. Mass Spectrom.* **1992**, *27*, 931.
(28) (a) Grese, R. P.; Cerny, R. L.; Gross, M. L. *J. Am. Chem. Soc.* **1989**, *111*, 2835. (b) Hu, P.; Gross, M. L. *J. Am. Chem. Soc.* **1993**, *115*, 8821. (c) Hu, P.; Sorensen, C.; Gross, M. L. *J. Am. Soc. Mass Spectrom.* **1995**, *6*, 1079. (d) Zhao, H.; Reiter, A.; Teesch, L. M.; Adams, J. *J. Am. Chem. Soc.* **1993**, *115*, 2854. (e) Reiter, A.; Adams, J.; Zhao, H. *J. Am. Chem. Soc.* **1994**, *116*, 7827. (f) Teesch, L. M.; Adams, J. *J. Am. Chem. Soc.* **1991**, *113*, 812. (g) Hofmeister, G.; Zhou, Z.; Leary, J. A. *J. Am. Chem. Soc.* **1991**, *113*, 5964.
(29) Gatlin, C. L.; Tureček, F.; Vaisar, T. *J. Mass Spectrom.* **1995**, *30*, 1605.
(30) (a) Cooks, R. G.; Kruger, T. L. *J. Am. Chem. Soc.* **1977**, *99*, 1279. (b) Mcluckey, S. A.; Cameron, D.; Cooks, R. G. *J. Am. Chem. Soc.* **1981**, *103*, 1313.
(31) (a) Cooks, R. G.; Patrick, J. S.; Kotiaho, T.; McLuckey, S. A. *Mass Spectrom. Rev.* **1994**, *13*, 287. (b) Wright, L. G.; McLuckey, S. A.; Cooks, R. G.; Wood, K. V. *Int. J. Mass Spectrom. Ion Processes* **1982**, *42*, 115. (c) Boand, G.; Houriet, R.; Gaumann, T. J. *J. Am. Chem. Soc.* **1983**, *105*, 2203. (d) Brodbelt, J. S.; Cooks, R. G. *Talanta* **1989**, *36*, 255.
(32) (a) Majumdar, T. K.; Clairet, F.; Tabet, J.-C.; Cooks, R. G. *J. Am. Chem. Soc.* **1992**, *114*, 2897. (b) Wu, Z.; Fenselau, C. *Rapid Commun. Mass Spectrom.* **1992**, *6*, 403. (c) Bojesen, G. *J. Am. Chem. Soc.* **1987**, *109*, 5557.
(33) McLuckey, S. A.; Schoen, A. E.; Cooks, R. G. *J. Am. Chem. Soc.* **1982**, *104*, 848.
(34) (a) Chen, L.-Z.; Miller, J. M. *Org. Mass Spectrom.* **1992**, *27*, 883. (b) Chen, L.-Z.; Miller, J. M. *J. Am. Soc. Mass Spectrom.* **1991**, *2*, 120.
(35) (a) Chen, L.-Z.; Miller, J. M. *J. Organomet. Chem.* **1993**, *448*, 225. (b) Kappes, M. M.; Staley, R. H. *J. Am. Chem. Soc.* **1982**, *104*, 1813. (c) Jones, R. W.; Staley, R. H. *J. Am. Chem.* Soc. **1982**, *104*, 2296.
(36) Strobel, F.; Ridge, D. P. *Inorg. Chem.* **1988**, *27*, 891.
(37) Becker, H.; Schröder, D.; Zummack, W.; Schwarz, H. *J. Am. Chem. Soc.* **1994**, *116*, 1096.
(38) Bojesen, G.; Breindahl, T.; Anderson, A. N. *Org. Mass Spectrum.* **1993**, *28*, 1448.
(39) Ceda, B. A.; Wesdemiotis, C. *J. Am. Chem. Soc.* **1995**, *117*, 9734.
(40) Hoke, S. H., II; Yang, S. S.; Cooks, R. G.; Hrovat, D. A.; Borden, W. T. *J. Am. Chem. Soc.* **1994**, *116*, 4888.
(41) Chen, G.; Kasthurikrishnan, N.; Cooks, R. G. *Int. J. Mass Spectrom. Ion Processes* **1995**, *151*, 69.
(42) Eberlin, M. N.; Kotiaho, T.; Shay, B. J.; Yang, S. S.; Cooks, R. G. *J. Am. Chem. Soc.* **1994**, *116*, 2457.
(43) Yang, S. S.; Bortolini, O.; Steinmetz, A.; Cooks, R. G. *J. Mass Spectrom.* **1995**, *30*, 184.
(44) Yang, S. S.; Chen, G.; Ma, S.; Cooks, R. G.; Gozzo, F.; Eberlin, M. N. *J. Mass Spectrom.* **1995**, *30*, 807.
(45) Yang, S. S.; Wong, P.; Ma, S.; Cooks, R. G. *J. Am. Soc. Mass Spectrom.* **1996**, 7, 198.
(46) Wong, P.; Ma, S.; Yang, S. S.; Cooks, R. G. *J. Am. Soc. Mass Spectrom.* Submitted for publication.
(47) (a) Liou, C. C.; Brodbelt, J. S. *J. Am. Chem. Soc.* **1992**, *114*, 6761. (b) Wu, H.-F.; Brodbelt, J. S. *J. Am. Soc. Mass Spectrom.* **1993**, *4*, 718.
(48) Cacace, F.; Petris, G. de; Pepi, F.; Angelelli, F. Submitted for publication.
(49) Schwarz, J. C.; Schey, K. L.; Cooks, R. G. *Int. J. Mass Spectrom. Ion Processes* **1990**, *101*, 1.
(50) Schwartz, J. C.; Wade, A. P.; Enke, C. G.; Cooks, R. G. *Anal. Chem.* **1990**, *62*, 1809.

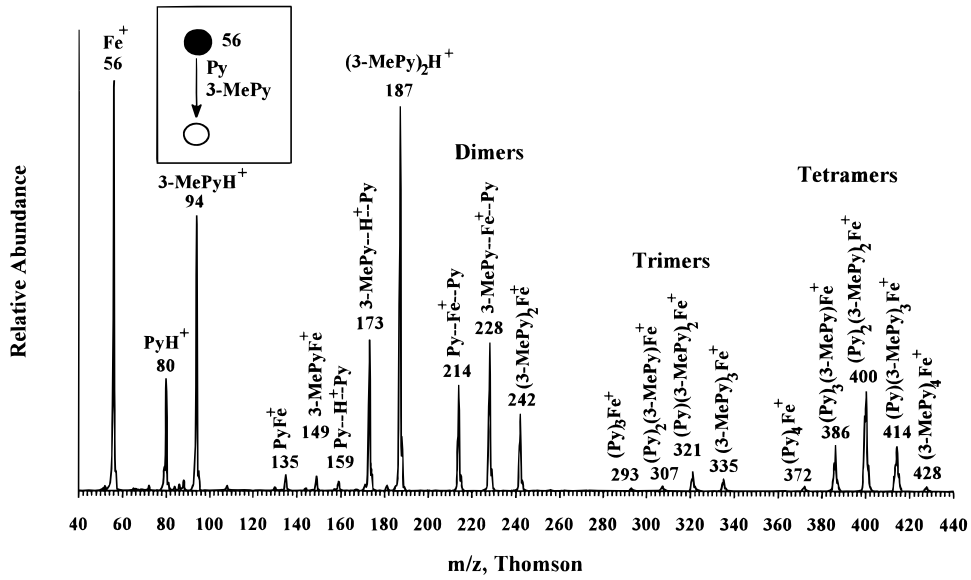

Figure 1. Reaction product spectrum displaying products of ion/molecule reactions of Fe^+ (56 Th) with a mixture of pyridine (Py) and 3-methylpyridine (3-MePy).

relative abundances of the two Fe^+-bound monomers and a knowledge of the effective temperature of the excited cluster ion.

One objective of this study is to compare Fe^+ bond strengths with pyridines to the strengths of the pyridine bonds with Cl^+, CN^+, $OCNCO^+$, $SiCl_3^+$, $SiCl^+$, and other cations. Another objective is to seek correlations between Fe^+ and other affinities as the substituents on the pyridine ligands are changed and a third is to compare steric effects in the various cation-bound clusters. The final aim is to compare molecular pair and molecular triplet Fe^+ affinities of substituted pyridines by studying dissociations of Fe^+-bound trimers and tetramers, respectively. In addition to measuring relative Fe^+ affinities of pyridines, the absolute value of Fe^+ affinity for pyridine is estimated using a reference compound of known Fe^+ affinity.

Experimental Section

Multiple-stage mass spectrometric (MS^2 and MS^3) experiments were performed in a pentaquadrupole mass spectrometer comprised of three mass-analyzing quadrupoles (Q1, Q3, and Q5) and two collision quadrupoles (Q2 and Q4). For the MS^2 experiments, mass-selected Fe^+ ions (Q1) were reacted with a vaporized mixture of two pyridines in Q2 at nominally zero collision energy. The reaction products were recorded by scanning Q5 while both Q3 and Q4 were operated in the RF-only mode. For the MS^3 experiments, the individual ion/molecule reaction products generated in Q2 were mass-selected in Q3 and subjected to collision-induced dissociation (CID) with argon as target gas in Q4, while Q5 was scanned to record the sequential product ion spectrum.[50]

The Fe^+ ion was generated by 70 eV electron ionization of iron pentacarbonyl (Aldrich Chemical Co., Milwaukee, WI) which was introduced into the ion source via a Granville Phillips leak valve (Granville Phillips Co., Boulder, CO) at a nominal pressure of 4×10^{-6} Torr, monitored by a single ionization gauge located near Q5. The pressure increased to 5×10^{-5} Torr on addition of a mixture of pyridines and rose further to 7×10^{-5} Torr upon addition of argon gas in Q4. The pyridines (Aldrich Chemical Co., Milwaukee, WI) are commercially available and were used as received. The nominal collision energy, the potential difference between the ion source and the collision quadrupole, was about 0 eV in Q2 for ion/molecule reactions and 10 eV in Q4 for CID experiments. Mass-to-charge ratios are reported using the Thomson unit (1 Th = 1 atomic mass per unit positive charge).[51]

Results and Discussion

Figure 1 shows a typical MS^2 ion/molecule reaction product spectrum for the reaction of mass-selected Fe^+, 56 Th, with a mixture of two pyridines, pyridine (Py) and 3-methylpyridine (3-MePy). Ion/molecule reactions lead to the formation of several products including the following: (i) the protonated monomers PyH^+, 80 Th, and $3\text{-}MePyH^+$, 94 Th; (ii) Fe^+-bound monomers, $PyFe^+$, 135 Th, and $3\text{-}MePyFe^+$, 149 Th; (iii) the proton-bound dimers, PyH^+Py, 159 Th, $PyH^+3\text{-}MePy$, 173 Th, and $3\text{-}MePyH^+3\text{-}MePy$, 187 Th; (iv) the two symmetrical Fe^+-bound dimers, $PyFe^+Py$, 214 Th, and $3\text{-}MePyFe^+3\text{-}MePy$, 242 Th; (v) the ion of most interest, the mixed dimer $PyFe^+3\text{-}MePy$, 228 Th; (vi) Fe^+-bound trimers, $(Py)_3Fe^+$, 293 Th, $(Py)_2Fe^+(3\text{-}MePy)$, 307 Th, $PyFe^+(3\text{-}MePy)_2$, 321 Th, and $(3\text{-}MePy)_3Fe^+$, 335 Th; and (vii) Fe^+-bound tetramers, $(Py)_4Fe^+$, 372 Th, $(Py)_3Fe^+(3\text{-}MePy)$, 386 Th, $(Py)_2Fe^+(3\text{-}MePy)_2$, 400 Th, $PyFe^+(3\text{-}MePy)_3$, 414 Th, and $(3\text{-}MePy)_4Fe^+$, 428 Th. The protonated pyridines and proton-bound dimers are probably formed via initial charge exchange of the pyridines with Fe^+ and subsequent proton transfer and association reactions.

Thermochemical Studies of the Dimers. The MS^3 sequential product spectrum of the unsymmetrical Fe^+-bound dimer, $(Py)Fe^+(3\text{-}MePy)$, 228 Th, was recorded to confirm its assignment as a loosely-bound dimer of this composition. The cluster ion was mass selected using Q3 and fragmented by collision-induced dissociation to produce the product spectrum shown in Figure 2. The only fragments observed under conditions of mild collisional activation, i.e. low energy (10 eV) and pressure (7×10^{-5} Torr), are the two Fe^+-bound monomers, $PyFe^+$, 135 Th, and $3\text{-}MePyFe^+$, 149 Th. This suggests that the dimers are loosely bound with the two pyridines attached to the central metal ion.[31]

The relative abundances of the two fragments in Figure 2 immediately suggest that 3-MePy has a higher Fe^+ affinity than pyridine. If the same electronic effects which influence proton affinities cause parallel effects in Fe^+ affinities, a linear relationship might be expected between $\ln(k_1/k_2)$, the logarithm of the relative dissociation rates, and the PAs of meta- or para-

(51) Cooks, R. G.; Rockwood, A. L. *Rapid Commum. Mass Spectrom.* **1991**, *5*, 93.

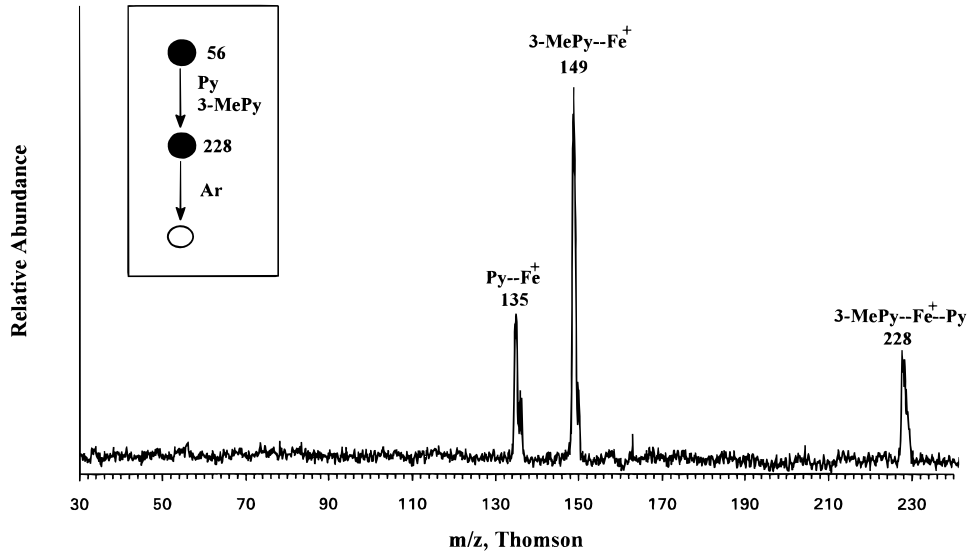

Figure 2. Sequential product (MS^3) spectrum showing fragmentation of the mixed dimer (228 Th) generated upon reaction of Fe^+ with a mixture of pyridine (Py) and 3-methylpyridine (3-MePy).

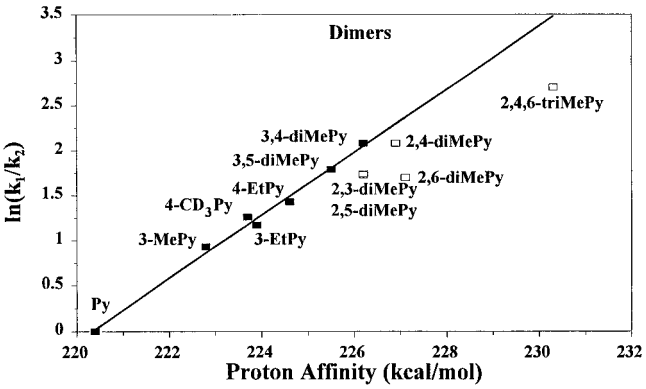

Figure 3. Linear correlation between $\ln([Py_1Fe]^+/[Py_2Fe]^+)$, which is proportional to the relative Fe^+ affinities of substituted pyridines, and the corresponding proton affinities. Open symbols represent ortho substituted pyridines which do not correlate due to steric effects.

substituted pyridines. As shown in Figure 3 such a relationship exists and it is described by

$$\ln(k_1/k_2) = 0.35\Delta PA \qquad (4)$$

According to the kinetic method, the logarithm of the ratio of relative abundances is directly proportional to the difference in the Fe^+ affinities of the two pyridines, as shown in eq 3. Therefore, it is possible to estimate the relative Fe^+ affinities using the quantity $\ln([Py_1Fe^+]/Py_2Fe^+])RT_{eff}$ if one knows the effective temperature for the activated dimers. A value of 555 K was estimated from AM1 calculations as the effective temperature of a large number of Cl^+-bound pyridine dimers[42] and a similar value (595 K) was estimated by the same method in a study of SF_3^+ affinities.[46] Given that all these experiments were performed under the same conditions, the value of 555 K is used here to estimate relative Fe^+ affinities. Note that the choice of effective temperature does not affect the existence of the correlation and that errors in the temperature of even 50 K correspond to changes in the relative affinities of only ±0.3 kcal/mol.[45] The results are summarized in Table 1. The order of relative Fe^+ affinities is Py < 3-MePy < 3-EtPy < 4-MePy < 4-EtPy < 3,5-Me_2Py < 3,4-Me_2Py, and the relative Fe^+ affinity values are linearly related to the relative proton affinities (ΔPA) by eq 5.

$$\text{relative } Fe^+ \text{ affinity} = 0.38\Delta PA \qquad (5)$$

In previous studies using pyridine dimers with $OCNCO^+$, $SiCl_3^+$, Cl^+, CN^+, and $SiCl^+$, linear correlations with ΔPA were also observed. The constants in these correlations are 0.96, 0.95, 0.83, 0.72, and 0.60, respectively. It seems reasonable to assume that the lower slopes correspond to smaller pyridine-cation bond strengths as suggested previously.[35] The small slope recorded for Fe^+ in this study, therefore, indicates that the binding between Fe^+ and pyridines is weaker than it is for the other cations listed. This may be due to the large size, the shielding effect of the 3d electrons and the diffuse nature of the 3d orbitals in Fe^+.

The absolute Fe^+-bond energy for pyridine is estimated using a reference compound, benzene, which has an Fe^+ affinity of 48.6 ± 2.0 kcal/mol as obtained recently by the kinetic method.[52] The cluster ion, 4-CD_3Py--Fe^+--C_6H_6, was therefore prepared and mass selected and then allowed to undergo collision-induced dissociation. The fragment ion abundance ratio ($[4\text{-}CD_3PyFe^+]/[C_6H_6Fe^+] = 5.3 \pm 0.5$) shows that the bond energy Fe^+-(4-CD_3Py) is 50.4 kcal/mol with an assumption of an effective temperature of 555 K. Hence, the bond energy of pyridine with Fe^+ is 49.0 kcal/mol with an estimated uncertainity of about ± 3 kcal/mol.

Thermochemical Studies of the Trimers. Dissociation of Fe^+-bound trimers containing two different pyridine molecules, abbreviated as A and B, occurs as shown in eq 6. The cluster ion A_2Fe^+B may fragment to A_2Fe^+ or to $ABFe^+$. The rate constant corresponding to loss of B is indicated as k_1' and that corresponding to loss of A is indicated as k_2'.

$$A_2Fe^+B \xrightarrow{k_1'} AFe^+A + B \qquad A_2Fe^+B \xrightarrow{k_2'} AFe^+B + A \qquad (6)$$

(52) (a) Seemeyer, K.; Hertwig, R. H.; Hrušák, J.; Koch, W.; Schwarz, H. *Organometallics* **1995**, *14*, 4409. (b) Schröder, D.; Schwarz, H. *J. Organomet. Chem*. In press.

(53) (a) Vékey, K.; Czira, G. *Rapid Commum. Mass Spectrom*. **1995**, *9*, 783. (b) Aue, D. H.; Bowers, M. T. In *Gas-Phase Ion Chemistry*; Bowers, M. T., Ed.; Academic Press: New York, 1979; Vol. 2.

Table 1. Relative and Absolute Fe^+ Affinities and Proton Affinities

entry	pyridines	Py_1:Py_2[a]	$\ln([Py_1Fe^+)]/[PyFe^+)])$[b]	Fe^+ affinity (kcal/mol) relative[c]	Fe^+ affinity (kcal/mol) absolute[d]	proton affinity[e] (kcal/mol)
1	Py		0	0	49.0	220.4
2	3-MePy	2:1	0.9	1.0	50.0	222.8
3	4-CD_3Py	3:1	1.3	1.4	50.4	223.7
4	3-EtPy	4:3	1.2	1.3	50.3	223.9
5	4-EtPy	5:3	1.4	1.6	50.6	224.6
6	3,5-Me_2Py	6:3	1.8	2.0	51.0	225.5
7	3,4-Me_2Py	7:3	2.1	2.3	51.3	226.2
8	2,5-Me_2Py	8:3	1.7	1.9	50.9	226.2
9	2,3-Me_2Py	9:3	1.7	1.9	50.9	226.2
10	2,4-Me_2Py	10:3	2.1	2.3	51.3	226.9
11	2,6-Me_2Py	11:3	1.7	1.9	50.9	227.1
12	2,4,6-Me_3Py	12:3	2.7	3.0	52.0	230.3

[a] The entry number of the pyridine forming the Fe^+-bound dimer used to estimate the Fe^+ affinities. [b] Experimental results. [c] Obtained from eq 3 (assuming $T_{eff} = 555$K); Fe^+ affinities are relative to pyridine. [d] Obtained by using benzene as the anchor point to compare its Fe^+ affinity (48.6 ± 2.0 kcal/mol)[52] with that of 4-CD_3Py. The Fe^+ affinities of the remaining compounds were then obtained by using the relative Fe^+ affinity measurements. The uncertainties in the Fe^+ affinities for pyridines are ±2.8 kcal/mol. [e] Proton affinities are taken from: Aue, D. H.; Bowers, M. T. In *Gas Phase Ion Chemistry*; Bowers, M. T., Ed.; Academic Press: New York, 1979, Vol. 2. This older set of values is used in preference to others because it is internally more consistent and it facilitates comparison of the present data with those for pyridine binding to other cations. See ref 45 for a discussion of this point.

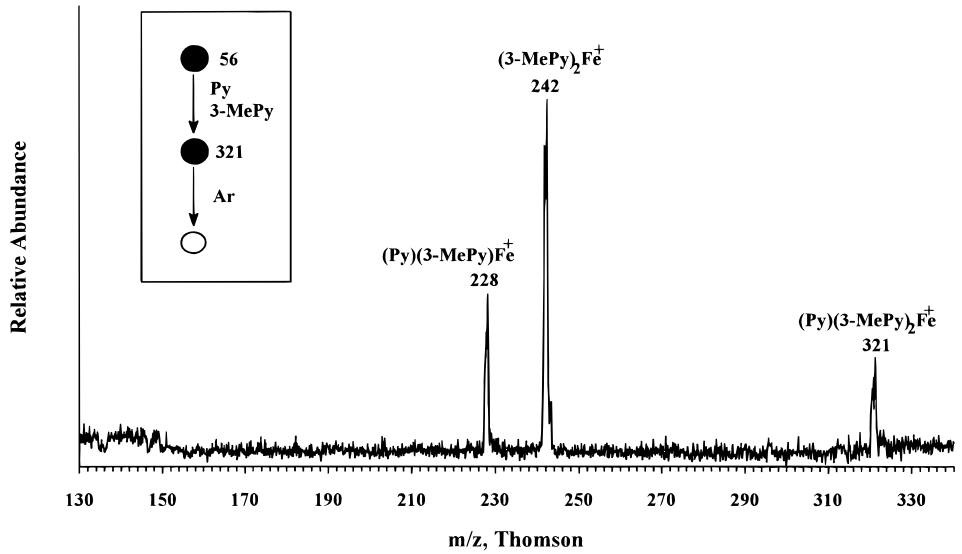

Figure 4. Sequential product (MS^3) spectrum showing fragmentation of the trimer, $PyFe^+(3\text{-MePy})_2$, 321Th, generated upon the ion−molecule reactions of Fe^+ with a mixture of pyridine and 3-methylpyridine.

If the kinetic method treatment applies, then using arguments analogous to those which yield eq 3, one gets

$$\ln \frac{k_1'}{k_2'} = \ln \frac{[A_2Fe]^+}{[AFeB]^+/2} = \frac{MPFeA(A_2) - MPFeA(AB)}{RT_{eff}} \quad (7)$$

where the molecular pair Fe^+ affinity, MPFeA(AB),[31a,53] is defined as $-\Delta H$ for the reaction

$$A + B + Fe^+ \rightarrow AFe^+B \quad (8)$$

and MPFeA(A_2), the molecular pair Fe^+ affinity of the dimer A_2, is the negative of the enthalpy change on addition of the two pyridine molecules to Fe^+ and T_{eff} is the effective temperature of the activated trimer, A_2Fe^+B. In the A_2Fe^+B cluster ion, any one of the three ligands may be cleaved; two of these yield AFe^+B and one gives AFe^+A, therefore the abundance of AFe^+B in eq 7 is divided by two to account for this statistical factor.[36,53] The lack of independently known MPFeA values and the difficulty in measuring the effective temperature of the trimers at present limits the application of the relationship in eq 7.

However, MS^3 studies of the Fe^+-bound trimers suggest they have loosely-bound structures. For example, the CID spectrum of $PyFe^+(3\text{-MePy})_2$ at 321 Th shows only two fragment ions and these correspond to the loss of one or the other ligand, Py or 3-MePy, with no further fragmentation (Figure 4). The ratio of rates of competitive dissociation is determined from the relative abundance of the two fragments using eq 7 and the values of k_1'/k_2' are listed in Table 2 for a series of pyridines. Note that for unhindered pyridines, values of k_1'/k_2' in the trimers are higher than the k_1/k_2 values for the dimers. This clearly indicates an accelerated loss of the most weakly-bound ligand as the number of ligands increases. This presumably occurs because each additional ligand weakens the Fe^+-ligand binding. Similar effects were observed by Strobel and Ridge.[36] In their study of $Fe(CO)_x(H_2O)^+$ where $x = 1$, 2, and 3, $\ln(k_1/k_2)$ was 0.7 when $x = 1$ and $\ln(k_1/k_2)$ increased to 1.5 and 1.8 when $x = 2$ and 3, respectively, where k_1 is the rate constant corresponding to loss of the ligand CO and k_2 is the rate constant corresponding to loss of the ligand H_2O. The relative loss of H_2O decreases more than is accounted for by the statistical effect of additional ligands, and the difference in the strengths of the H_2O and CO bonds with the metal ion Fe^+ increases substan-

Table 2. Effect of Cluster Size on the Ratio of the Dissociation Rate Constants

entry	pyridines	A:B[a]	k_1/k_2[b] dimer	k_1'/k_2' [c] trimer	k_1''/k_2'' [d] tetramer	ΔPA (A−B)
1	Py					
2	3-MePy	2:1	2.5	4.0	3.2	2.4
				3.9	3.8	
					4.0	
3	4-CD_3Py	3:1	3.4	5.3	5.3	3.3
				5.8	5.8	
					6.6	
4	3-EtPy	4:3	0.9	0.7	1.1	0.2
				0.8	1.0	
					1.0	
5	4-EtPy	5:3	1.2	1.5	1.4	0.9
				1.3	1.6	
					1.7	
6	3,5-Me_2Py	6:3	1.7	2.4	3.1	1.8
				2.5	2.3	
					2.5	
7	3,4-Me_2Py	7:3	2.3	4.1	4.0	2.5
				4.1	4.1	
					3.7	
8	2,5-Me_2Py	8:3	1.6	1.5	1.5	2.5
				1.5	1.5	
					1.4	
9	2,3-Me_2Py	9:3	1.6	1.1	1.1	2.5
				1.1	1.1	
					1.0	
10	2,4-Me_2Py	10:3	2.3	2.7	2.7	3.2
				2.7	1.9	
					1.9	
11	2,6-Me_2Py	11:3	1.6	0.8	1.0	3.4
				0.8	0.8	
12	2,4,6-Me_3Py	12:3	4.2	3.5	3.8	6.6
				2.5		

[a] The entry number of the pyridines forming the Fe^+-bound cluster used to estimate the ratio of unimolecular dissociation rate constants. [b] k_1/k_2 = $[AFe^+]/[BFe^+]$. [c] First row: k_1'/k_2' = $[ABFe^+]/2[B_2Fe^+]$. Second row: k_1'/k_2' = $2[A_2Fe^+]/[ABFe^+]$. [d] First row: k_1''/k_2'' = $[AB_2Fe^+]/3[B_3Fe^+]$. Second row: k_1''/k_2'' = $[A_2BFe^+]/[AB_2Fe^+]$. Third row: k_1''/k_2'' = $3[A_3Fe^+]/[A_2BFe^+]$. Relative standard deviation (3 measurements) ∼ ±10%.

tially as the number of CO ligands increases. This suggests that the additional CO ligands weaken the Fe^+−CO bond and accelerate the loss of CO ligand. It is gratifying to note that values of k_1'/k_2' in the two unsymmetrical trimers, $PyFe^+$(3-MePy)$_2$ and $(Py)_2Fe^+$(3-MePy), agree within experimental error. Similar values are also observed between A_2Fe^+B and AFe^+B_2 for other pairs of unhindered pyridines, as shown in Table 2. These results, which are given in terms of ion abundance ratios rather than log ratios in order to facilitate their intercomparison, show that the number rather than the type of ligands principally determines the Fe^+−ligand bond dissociation energy.

If the effects which influence molecular pair proton affinity (MPPA) also affect MPFeA, a linear relationship is expected between $\ln(k_1'/k_2')$ and the MPPA of the unhindered pyridine pairs. Unfortunately, there is relatively little known regarding the MPPA values of pyridines. However, the values of k_1'/k_2' are observed to be dependent on the proton affinity difference of the ligands and a linear correlation is observed between the average $\ln(k_1'/k_2')$ values of the trimers and ΔPA values (Figure 5). This relationship, which is limited to pyridines without ortho substituents, is of the form

$$\ln(k_1'/k_2') = 0.53\Delta\mathrm{PA} \qquad (9)$$

That ortho substituents on the pyridines weaken the binding to the central Fe^+ ion is evident not only from the deviations which occur in the kinetic method plot for the dimers (Figure

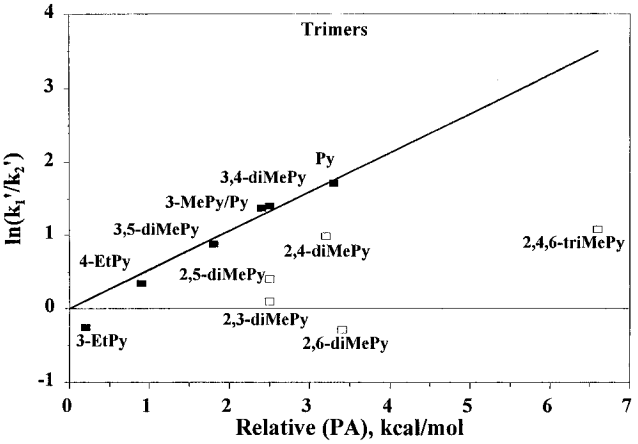

Figure 5. Linear correlation between $\ln(k_1'/k_2')$, the competitive rates of dissociation of the Fe^+-bound trimers and the relative proton affinities. Open symbols represent ortho substituted pyridines which do not correlate due to steric effects.

3) but also in the rate data for the trimers and tetramers in Table 2. In contrast to the general increase in the ratios seen in the series dimers < trimers < tetramers, for meta- or para-substituted pyridines, the ortho-substituted systems **8**−**12** generally show a decrease in this ratio. The increase in the non-ortho-substituted series is attributed to the decreased importance of binding by the most weakly-bound ligand as the number of ligands increases. The decrease in the ratio for the ortho-substituted systems is attributed to the enhanced steric effects in the more crowded trimers and tetramers, which weakens all binding and so attenuates the differences between the ligands. Both these effects are discussed in detail below.

The relative MPFeAs for pyridine dimers can be estimated using eq 7 provided an assumption is made regarding the effective temperature for the activated trimer. Ridge and co-workers[36] used the same effective temperature for the dimer, trimer, and tetramer in their studies of $Fe(CO)_x(H_2O)^+$ (x = 1, 2, and 3, respectively). Following suit, we assume that the Fe^+-bound trimers and tetramers have the same effective temperature as the Fe^+-bound dimers for which the value of 555 K is assumed (see above). Even though this assumption is a rough approximation, the relative MPFeA will not change by more than 0.4 kcal/mol with a change of 50 K in effective temperature. The MPFeA values derived from the study of the pyridine trimers are listed in Table 3. Perusal of the relative MPFeA values shows trends which are analogous to those observed for the relative Fe^+ affinities (Table 1). For example, there is a close correspondence between the relative Fe^+ affinities (Table 1) and the relative MPFeA (A_2) affinities (Table 3).

Thermochemical Studies of the Tetramers. MS^3 studies show that the Fe^+-bound tetramers are also loosely bound and fragment readily and exclusively by loss of intact pyridine ligands. For example, $A_2Fe^+B_2$ fragments to A_2Fe^+B or AFe^+B_2 by loss of either ligand A or B and the product ions fragment further to give Fe^+-bound dimers, as shown in eq 10.

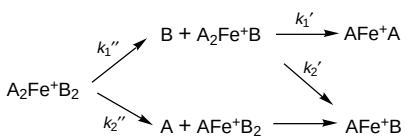

(10)

For example, the CID spectrum of the unsymmetrical tetramer, $(Py)_2Fe^+$(3-MePy)$_2$, 400 Th, gives two Fe^+-bound trimers which fragment further to the several dimers under mild activation conditions (10 eV collision energy) as shown in Figure 6.

Table 3. Relative Molecular Pair and Molecular Triplet Fe^+ Affinities of Pyridine Dimers and Trimers

			relative MPFeA[b]			relative MTFeA[c]			
entry	pyridines	A:B[a]	A_2	AB	B_2	A_3	A_2B	AB_2	B_3
1	Py		0			0			
2	3-MePy	2:1	3.0	1.5	0	4.3	2.8	1.3	0
3	4-CD_3Py	3:1	3.8	1.8	0	5.9	3.8	1.8	0
4	3-EtPy	4:3	3.1	3.4	3.8	5.9	5.9	6.0	5.9
5	4-EtPy	5:3	4.5	4.2	3.8	7.3	6.8	6.2	5.9
6	3,5-Me_2Py	6:3	5.8	4.7	3.8	9.0	8.0	7.1	5.9
7	3,4-Me_2Py	7:3	6.9	5.3	3.8	10.4	9.0	7.4	5.9
8	2,5-Me_2Py	8:3	4.7	4.2	3.8	7.1	6.8	6.3	5.9
9	2,3-Me_2Py	9:3	4.0	3.9	3.8	6.1	6.1	6.0	5.9
10	2,4-Me_2Py	10:3	6.0	4.9	3.8	8.4	7.7	7.0	5.9
11	2,6-Me_2Py	11:3	3.3	3.5	3.8		5.6	5.9	5.9
12	2,4,6-Me_3Py	12:3	6.2	5.2	3.8			7.3	5.9

[a] The entry number of the pyridines forming the Fe^+-bound clusters used to estimate MPFeA values and MTFeA values for dimers and trimers. [b] Molecular pair Fe^+ affinity, obtained from eq 7. MPFeA values are given in kcal/mol relative to MPFeA(Py_2). [c] Molecular triplet Fe^+ affinity, obtained from eq 11. MTFeAs are relative to MTFeA(Py_3).

Application of the kinetic method to this type of cluster ion requires that further dissociations do not occur to a significant extent[30,31] and therefore, in order to estimate k_1''/k_2'' values for the tetramers, it is necessary to "add back" the abundances of secondary fragments to the abundances of the parent trimers. This can be done on the assumption that the secondary fragmentation is a sequential process and that the k_1'/k_2' values are the same as those determined from the direct fragmentation of the mass-selected trimers. By comparing the k_1'/k_2' value in a trimer which displays no further fragmentation with the k_1'/k_2' value showing secondary fragmentation to the monomers, these assumptions can be tested. The pressure of argon collision gas was increased in the collision-induced dissociation of a mass-selected trimer, (3-MePy)$Fe^+(Py)_2$, 307 Th, until the onset of secondary fragmentation to yield the monomers occurred (nominal pressure $= 1.5 \times 10^{-4}$ Torr). By adding the abundance of monomers back to those of the dimers, the k_1'/k_2' value was calculated to be 3.8 using the same assumptions discussed above, which is close to the value of 4.0 obtained from the dissociation of the same trimer under conditions with no further fragmentation. On the other hand, if the monomers are considered to be formed directly from the trimer, the k_1'/k_2' value (3.0) becomes significantly smaller than the experimental value (4.0). This result demonstrates that further fragmentation indeed occurs in the tetramer via a sequential process, as expected.

The k_1''/k_2'' values for the tetramers are displayed in Table 2 for the series of pyridines studied. The values of $\ln(k_1''/k_2'')$ are related to the difference in molecular triplet Fe^+ affinities of the trimers,

$$\ln \frac{k_1''}{k_2''} = \ln \frac{[A_2FeB]^+/2}{[AFeB_2]^+/2} = \frac{\text{MTFeA}(A_2B) - \text{MTFeA}(AB_2)}{RT_{\text{eff}}} \quad (11)$$

where the molecular triplet Fe^+ affinity MTFeA (ABC) is defined as $-\Delta H$ for the reaction

$$A + B + C + Fe^+ \rightarrow ABCFe^+ \quad (12)$$

Since the molecular triplet proton affinities for the trimers are not available (indeed no molecular triplet affinities of any type appear to have been reported), the $\ln(k_1''/k_2'')$ values are plotted versus ΔPA, as shown in Figure 7. The good correlation observed provides further evidence that the assumptions underlying this treatment are sound. The correlation can be expressed as

$$\ln(k_1''/k_2'') = 0.54\Delta\text{PA} \quad (13)$$

The order of the relative MTFeA values of the trimers, expressed as $\ln[k_1''/k_2'']RT_{\text{eff}}$, using eq 11 is displayed in Table 3. These data show a good correspondence with the MPFeA values.

It has been shown that the relative Fe^+ affinities correlate linearly with the proton affinities of pyridines (Figure 3). The relative MPFeA and MTFeA values also correlate very well (Figures 8 and 9) with a new quantity, the *number averaged proton affinities* of the meta- and para-substituted pyridines, defined by the following equation:

$$\text{number averaged PA}(A_mB_n) = \frac{m\text{PA(A)} + n\text{PA(B)}}{m+n} \quad (14)$$

For example, the number averaged PA of (3-MePy, 3-MePy, Py) is $(2 \times 222.8 + 220.4)/3 = 222.0$ kcal/mol. The linear relationships can then be expressed (in kcal/mol) as

$$\text{relative MPFeA} = 1.1359(\text{no. av PA}) - 250.42 \quad (15)$$

$$\text{relative MTFeA} = 1.7973(\text{no. av PA}) - 396.24 \quad (16)$$

Equations 15 and 16 can be used to estimate and predict molecular pair and molecular triplet Fe^+ affinities from a knowledge of proton affinities.

Quantitative Treatment of the Dissociation Rates. The relative dissociation rates of dimers, trimers, and tetramers of unhindered pyridines, expressed in terms of the relative abundances of the fragment ions, are shown in eqs 4, 9, and 13. A simplified potential energy diagram is used to demonstrate the relationships between the various dissociation channels (Figure 10). Species A represents a molecule with higher Fe^+ affinity than species B. Examination of Figure 10 shows that the relative rates of dissociation for a dimer, A---Fe^+---B, can be expressed as

$$\ln \frac{k_1}{k_2} = \frac{\Delta_1}{RT_{\text{eff}}} = \frac{D_1 - D_2}{RT_{\text{eff}}} = 0.35\Delta\text{PA} \quad (17)$$

Applying a similar analysis to the trimers, A_2---Fe^+---B, gives

$$\ln \frac{k_1'}{k_2'} = \frac{\Delta_2}{RT_{\text{eff}}} = \frac{(D_1 - D_2) + (D_3 - D_4)}{RT_{\text{eff}}} = 0.53\Delta\text{PA} \quad (18)$$

Considering a tetramer, A_3---Fe^+---B, one can deduce that

$$\ln \frac{k_1''}{k_2''} = \frac{\Delta_3}{RT_{\text{eff}}} = \frac{(D_1 - D_2) + (D_3 - D_4) + (D_5 - D_6)}{RT_{\text{eff}}} = 0.54\Delta\text{PA} \quad (19)$$

From eqs 17, 18, and 19, one can easily deduce that

$$D_1 - D_2 = 0.35RT_{\text{eff}}\Delta\text{PA} \quad (20)$$

$$D_3 - D_4 = 0.18RT_{\text{eff}}\Delta\text{PA} \quad (21)$$

$$D_5 - D_6 = 0.01RT_{\text{eff}}\Delta\text{PA} \quad (22)$$

where D_1, D_2, D_3, D_4, D_5, and D_6 are the respective bond dissociation energies (BDE) of Fe^+--A, Fe^+--B, AFe^+--A, BFe^+--A, A_2Fe^+--A, and $ABFe^+$--A. The order $(D_1 - D_2) > (D_3 - D_4) \gg (D_5 - D_6)$ is expected. This can be understood from the fact that $(D_1 - D_2)$ is the difference in bond dissociation

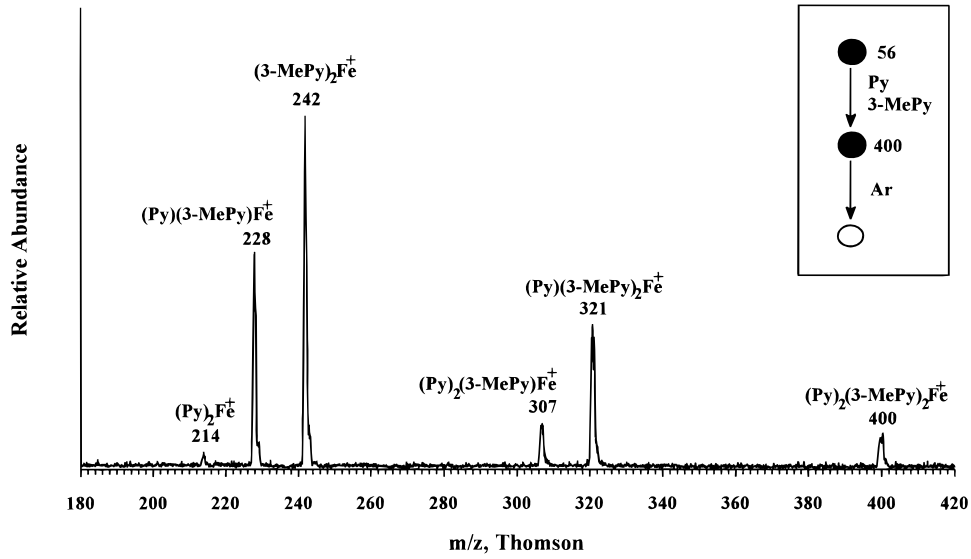

Figure 6. Sequential product spectrum of Fe^+-bound tetramer, $(Py)_2Fe^+(3\text{-}MePy)_2$, 400 Th, generated upon reaction of Fe^+ with a mixture of pyridine and 3-methylpyridine.

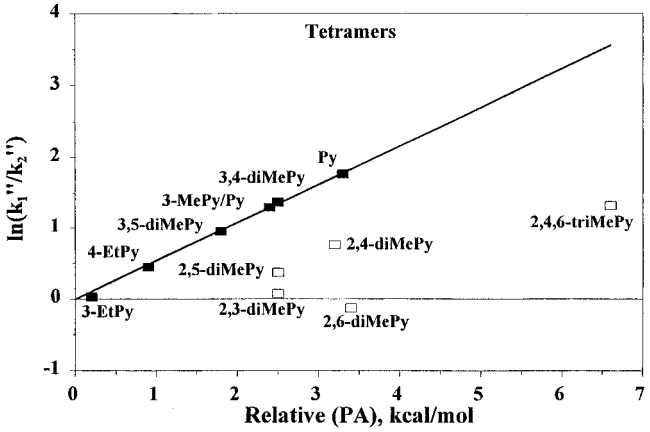

Figure 7. Linear correlation between $\ln(k_1''/k_2'')$, the competitive rates of dissociation of the Fe^+-bound tetramers, and the relative proton affinities. Open symbols represent ortho-substituted pyridines which do not correlate due to steric effects.

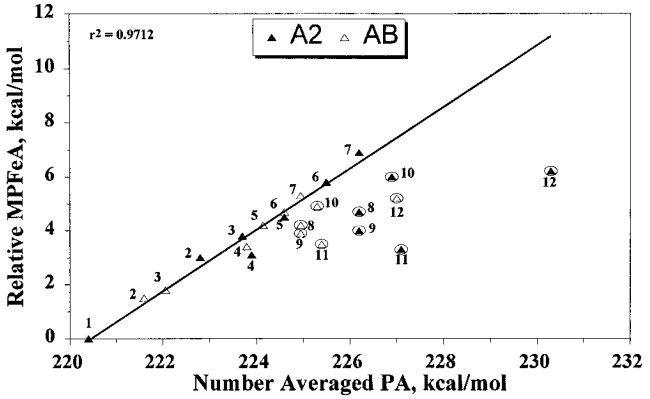

Figure 8. Linear correlation between relative molecular pair Fe^+ affinities (MPFeA) and the number averaged proton affinities of the pyridine dimers. The numbers are the entry numbers of the pyridines in Table 3. Open circles represent ortho-substituted pyridines which show steric effects.

energies between Fe^+--A and Fe^+--B, while $(D_3 - D_4)$ is the difference in bond dissociation energy between AFe^+--A and BFe^+--A (i.e. cleaving the same ligand A from the dimers A_2-Fe^+ and AFe^+B). Therefore, the difference in Fe^+ affinities of A and B has less effect on the cleavage in the dimer than it has

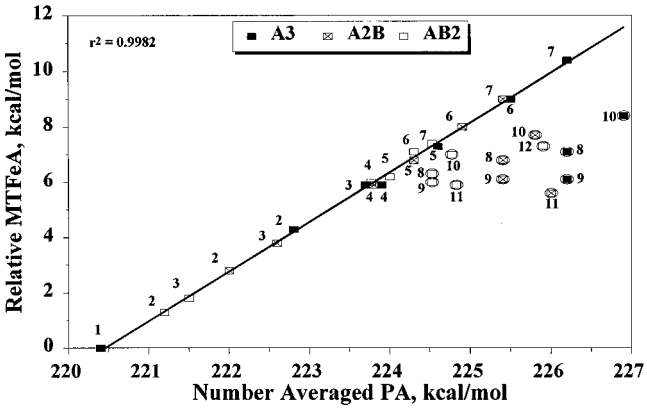

Figure 9. Linear correlation between relative molecular triplet Fe^+ affinities (MTFeA) and the number averaged proton affinities of the pyridine trimers. The numbers are the entry numbers in Table 3. Open circles represent ortho-substituted pyridines which show steric effects.

in the monomer and results in a smaller difference in bond dissociation energy. Similarly, the difference in bond dissociation energy $(D_5 - D_6)$ between A_2Fe^+--A and $ABFe^+$--A (i.e. cleaving the same ligand A from the trimers A_3Fe^+ and A_2-Fe^+B) is expected to be very small. As the number of ligands A bonded to Fe^+ increases, it is obvious that both the Fe^+-A and Fe^+-B bond dissociation energies decrease and the difference in bond dissociation energy between A_nFe^+--A and $A_{n-1}BFe^+$--A tends to zero.

Steric Parameters. Although the correlation between the relative Fe^+ affinities and proton affinities for these unhindered pyridines is excellent, it is poor for ortho-substituted pyridines. Figure 3 shows a lower than expected Fe^+ affinity for pyridines with ortho substituents. Such behavior can best be understood as being the result of steric effects arising from the ortho substituents. Steric hindrance might cause a lengthening of the N--Fe^+ bond which consequently decreases its strength and decreases the Fe^+ affinities of the hindered pyridines.

The steric effects of ortho groups not only reduce the observed values of relative Fe^+ affinities, but in a few cases also cause inversions when the affinities are compared with the PA order. For example, proton affinities for the dimethyl-substituted pyridines can be ordered as follows: 2,6-Me_2Py > 2,4-Me_2Py > 2,3-Me_2Py = 2,5-Me_2Py = 3,4-Me_2Py > 3,5-Me_2Py (Table 1). Since the *o*- and *p*-methyl groups have very similar

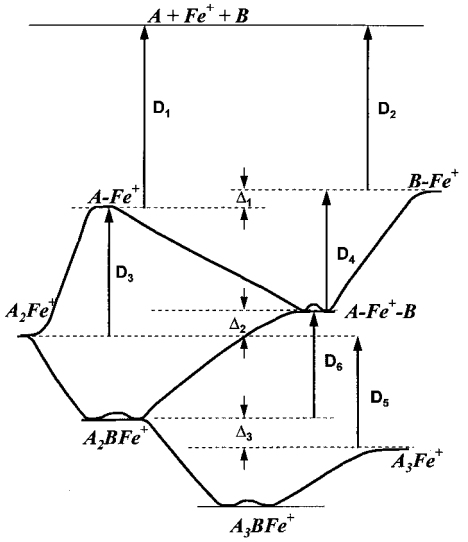

Figure 10. Potential energy surface diagram for the unimolecular dissociation of an Fe^+-bound tetramer, trimer, and dimer. Molecule A has a higher Fe^+ affinity than B. Note that $D_1 > D_3 > D_5$, $D_2 > D_4 > D_6$, and $\Delta_3 > \Delta_2 > \Delta_1$.

Table 4. Steric Parameters S^k for Ortho-Substituted Pyridines in Fe^+-Bound Dimers

	$\ln\{[Py_1Fe^+]/[Py_2Fe^+]\}$		
pyridine	exptl	calcd[a]	S^k [b]
2,4-Me_2Py	2.1	2.3	−0.2
2,5-Me_2Py	1.7	2.0	−0.3
2,3-Me_2Py	1.7	2.0	−0.3
2,6-Me_2Py	1.7	2.4	−0.7
2,4,6-Me_3Py	2.7	3.5	−0.8

[a] Calculated data from the linear regression eq 4. [b] S^k is the difference between the experimental data and the calculated data. It represents the combined steric effects of the groups contained in the cluster ion.

electronic effects on the pyridine molecules, and these effects are larger than those of *m*-methyl groups, 2,6-dimethylpyridine shows the greatest proton affinity. However, the steric hindrance of the two *o*-methyl groups gives this compound the lowest Fe^+ affinity value among the dimethyl-substituted pyridines (Figure 3). In addition, 2,4-dimethylpyridine shows a Fe^+ affinity approximately equal to that of 3,4-dimethylpyridine although the PA of 2,4-dimethylpyridine is 0.7 kcal/mol greater than that of 3,4-dimethylpyridine.

Quantitative studies of steric effects of substituents must separate these effects from electronic effects.[54] Note that the ratios of the two fragment ions of Fe^+-bound dimers containing unhindered pyridines are very similar to those in proton-bound dimers. It is reasonable to suggest that, when a pair consisting of a steric ortho-substituted pyridine (Py^h) and an unhindered pyridine (Py^u) is studied, the deviation of the experimentally measured logarithm of relative dissociation rates ($\ln([Py^hFe]^+/[Py^uFe]^+)$) from the value predicted by linear regression using results from para- and meta-substituted pyridines is due to the steric effect of the ortho group. This deviation is defined as the value of the gas-phase steric parameter S^k.[42] Using this definition, steric effects of several hindered pyridines were determined and the results are displayed in Table 4. Very large intramolecular steric effects are observed in 2,6-dimethylpyridine and 2,4,6-trimethylpyridine, both of which contain two methyl groups in the ortho position ($S^k = -0.7$ and -0.8, respectively). These values are more than twice as large as those for compounds containing only one *o*-methyl group ($S^k = -0.2$ for 2,4-dimethylpyridine and -0.3 for both 2,3-dimethylpyridine and 2,5-dimethylpyridine). This enhanced effect can be explained by the fact that the higher Fe^+ affinities of 2,6-Me_2Py and 2,4,6-Me_3Py shorten the bond lengths between the substituted pyridines and the Fe^+ cation, thereby increasing (buttressing) the steric effects.

(54) (a) Gallo, R.; Roussel, C.; Berg. U. In *Advances in Heterocyclic Chemistry*; Katritzky, A. R., Ed.; Academic Press: New York, 1988; Vol. 43, p 173. (b) Berg, U.; Gallo, R.; Klatte, G.; Metzger, J. *J. Chem. Soc., Perkin Trans. 2* **1980**, 1350.

Table 5. Steric parameters $S^{k\prime}$ for Ortho-Substituted Pyridines in Fe^+-Bound Clusters

		steric parameters, $S^{k\prime}$ [a]				
		trimers		tetramers		
pyridine, A	pyridine, B	A_2B	AB_2	A_3B	A_2B_2	AB_3
2,4-Me_2Py	4-CD_3Py	−1.2	−0.5	−3.2	−1.9	−0.7
2,5-Me_2Py	4-CD_3Py	−1.7	−0.8	−3.2	−2.1	−1.0
2,3-Me_2Py	4-CD_3Py	−2.3	−1.1	−4.2	−2.8	−1.3
2,6-Me_2Py	4-CD_3Py	−3.9	−1.9		−4.4	−1.9
2,4,6-Me_3Py	4-CD_3Py	−4.5	−2.0			−2.5

[a] $S^{k\prime}$ value is the difference between the experimental data and the calculated data from the linear regression lines in Figures 8 and 9 and divided by RT_{eff}. It represents the combined steric effects of the groups contained in the cluster ion.

Steric parameters also depend on the size of the central cation. Steric effects are expected to be negligible in proton-bound dimers owing to the very small size of the proton. Comparison of the steric parameters of 2,3-dimethylpyridine in Cl^+-bound dimer ($S^k = -0.64$),[42] $OCNCO^+$-bound dimer ($S^k = -3.29$),[44] $SiCl_3^+$-bound dimer ($S^k = -0.22$),[45] SF_3^+-bound dimer ($S^k = -2.15$),[46] and Fe^+-bound dimer ($S^k = -0.3$) demonstrates that the Fe^+ system has a similar steric effect to that of the $SiCl_3^+$ system, but much smaller effects than that in the bulky $[OCNCO]^+$ and SF_3^+ systems. The large steric parameter in the SF_3^+ system is ascribed to the lone pair of electrons on the sulfur which may repel the ortho substituent(s) and decrease the bond strength.[46] The modest-sized steric effects in Fe^+ are consistent with the proposal that relatively long and weak bonds are involved.

Lower than expected relative MPFeA and MTFeA values are also found for the ortho-substituted pyridines when the dissociation of trimers and tetramers is examined, and this too must be due to steric effects. The steric effects of individual pyridines in trimers and tetramers can be estimated from the deviation of the experimental data from the regression lines in Figures 8 and 9. (Note that all the points which lie off the line are for clusters which contain ortho-substituted pyridines.) The results are listed in Table 5. The steric effect for clusters which contain ortho-substituted pyridines increases in the order 2,4-Me_2Py < 2,5-Me_2Py < 2,3-Me_2Py < 2,6-Me_2Py < 2,4,6-Me_3Py. This order is the same for the dimers (Table 4) and for the two types of trimers and three types of tetramers examined. (The trimers are of the type A_2B and AB_2 and tetramers A_3B, A_2B_2, and AB_3 where A is a sterically hindered pyridine and B is 4-methyl-d_3-pyridine.) It is observed that the steric effects in general increase in the order $A_3B > A_2B_2 > AB_3$ as well as $A_2B > AB_2$. For example, the steric parameter for the 4-CD_3Py/2,4-Me_2Py dimer ($S^{k\prime} = -0.2$) is significantly lower than that for the trimer containing 2,4-Me_2Py and two 4-CD_3Py ($S^{k\prime} = -0.5$) due to the more crowded environment in the trimer. A much higher steric effect ($S^k = -1.2$) is observed for the trimer containing two 2,4-Me_2Py ligands and a 4-CD_3Py. The steric effect in the tetramers is higher still than that in the trimers. It is generally observed that the overall steric parameter increases as the number of hindered pyridines increases or as the total number of pyridine ligands increases. Overall, the steric

parameter is ordered as follows: $A_3B > A_2B_2 > A_2B > AB_3 > AB_2 > AB$. Note that these S^k parameters describe the combined steric effects in the whole cluster ion. Parameters for individual pyridines can be estimated by additivity. The results bear out the above generalizations, viz. the steric effect of a group increases in the order 2,4-Me_2Py < 2,5-Me_2Py < 2,3-Me_2Py < 2,6-Me_2Py < 2,4,6-Me_3Py and the effect of each group increases with the cluster size.

Conclusion

The Fe^+−pyridine bond is representative of those encountered in many other systems of interest in metal ion chemistry, especially in those encountered in the increasing number of studies which use metal ions as chemical ionization reagents in structural studies on biological compounds. Trends have been found in the strength of this bond with the degree of substitution on the pyridine and with the number of pyridine ligands coordinated to a single Fe^+ ion. The decrease in ligand bond dissociation energy as more ligands are added parallels trends observed much earlier for solvated alkali metal ions.[55,56] Remarkably, the Fe^+/pyridine bond energies parallel those of the pyridine−proton bond, except when steric interactions occur. This is evident from the excellent linear correlation (slope = 0.38) which exists between the relative Fe^+ affinities and the corresponding proton affinities. Other cations, including polyatomic ions such as $OCNCO^+$, also show this simple relationship. The fact that Fe^+ displays the weakest binding to pyridines among a variety of cations studied ($OCNCO^+ \approx SiCl_3^+ > Cl^+ > CN^+ > SiCl^+ > Fe^+$) is rationalized in terms of its large size, the shielding effect of the 3d electrons, and the diffuse nature of the 3d orbitals in Fe^+.

With a recent study by Vékey *et al.*,[53] this is the first use of the kinetic method to study molecular pair affinities: it is also the first systematic study of molecular pair affinities of a cation other than the proton and the first study of molecular triplet affinities of any ion by the kinetic method. These techniques are used to show that Fe^+-bound dimeric, trimeric, and tetrameric clusters all behave remarkably similarly; although the bond strengths are attenuated in the larger clusters, the underlying electronic effects are those that operate in protonated pyridine. The relative MPFeA values for pyridine dimers and MTFeA values for trimers are ordered from studies of the dissociation of Fe^+-bound trimers and tetramers and internal consistency in these values is shown, as is a good correlation with the number averaged proton affinities of the unhindered pyridines. This correlation is used to estimate molecular pair and molecular triplet affinities. The high relative rates of dissociation found in trimers (k_1'/k_2') and tetramers (k_1''/k_2'') compared with that in dimers (k_1/k_2) indicates an accelerated loss of the more weakly bound ligands as the number of ligands increases. This shows a strong ligand effect on the metal ion−ligand bond strength and the trends observed in this study parallel the trends observed for successive solvation energies of the proton, alkali metal ions, and halide ions.[55,56]

Steric effects are observed in Fe^+-bound dimers, trimers, and tetramers containing ortho-substituted groups. The steric effects decrease the Fe^+ affinities through repulsive interactions between the Fe^+ cation and the ortho substituent(s). The gas-phase steric parameters for ortho-substituted pyridines are similar to those found in the $SiCl_3^+$ system but are much smaller than those for the corresponding $OCNCO^+$ system. Steric parameters are generally larger in tetramers than those in trimers and dimers and increase with the number of hindered pyridines in the cluster ion.

Acknowledgment. This work was supported by the National Science Foundation, CHE 92-23791. P.W. thanks Eli Lilly and Company for Fellowship support.

JA954167H

(55) (a) Klassen, J. S.; Blades, A. T.; Kebarle, P. *J. Am. Chem. Soc.* **1994**, *116*, 12075. (b) Klassen, J. S.; Blades, A. T.; Kebarle, P. *J. Phys. Chem.* **1995**, *99*, 15509. (c) Blades, A. T.; Klassen, J. S.; Kebarle, P. *J. Am. Chem. Soc.* **1995**, *117*, 10563. (d) Anderson, S. G.; Blades, A. T.; Klassen, J.; Kebarle, P. *Int. J. Mass Spectrom. Ion Processes* **1995**, *141*, 217.

(56) Castleman, A. W., Jr. In *Clusters of Atoms and Molecules II*; Haberland, H., Ed.; Springer-Verlag: New York, 1994; p 77.